CONF-960613--1
SAND96-0778C

MULTI-SPECTRAL PUSHBROOM IMAGING RADIOMETER (MPIR) FOR REMOTE SENSING STUDIES*

Gary S. Phipps and Carter L. Grotbeck
Sandia National Laboratories
Albuquerque, New Mexico 87185-0980, USA
Telephone: (505) 845-8269
FAX: (505) 844-2057

RECEIVED
APR 0 1 1996
OSTI

ABSTRACT

A Multi-spectral Pushbroom Imaging Radiometer (MPIR) has been developed as a well-calibrated, imaging radiometer for studies of cloud properties from an Unmanned Aerospace Vehicle (UAV) platform. The instrument is designed to fly at altitudes up to 20 km and produce data from nine spectral detector modules. Each module has its own telescope optics, linear detector array, spectral filter, and necessary electronics. Cryogenic cooling for the long-wavelength infrared modules, as well as temperature regulation of the short-wavelength modules, is provided by a liquid nitrogen system designed to operate for multi-day missions. Pre- and post-flight calibration, combined with an on-board calibration chopper provide an instrument with state-of-the-art radiometric measurement accuracies. Each module has a ±40° across-track field-of-view and images a curved footprint onto its linear detector array. The long-wavelength array types have 256 detector elements while the short-wavelength arrays can have 512 elements. A modular design allows individual spectral bands to be changed to match the requirements for a particular mission.

1.0 INTRODUCTION

The Multi-spectral Pushbroom Imaging Radiometer (MPIR) is designed as a well-calibrated imaging radiometer for aircraft studies of cloud properties. The small size and weight allow operation from an Unmanned Aerospace Vehicle (UAV) platform at altitudes from the surface up to 20 km. The sensor has been developed as part of the DOE's Atmospheric Radiation Measurements (ARM) program. The ARM program seeks to obtain improved understanding of the earth and its atmosphere in response to global change. Improved measurements of cloud properties and water vapor profiles are critical to understanding a key global change issue: the role of radiation-cloud interactions on the earth's radiation budget. These parameters are also of high priority to the DoD for improved atmospheric and near space weather forecasting, for predicting infrared backgrounds for surveillance and weapon systems, for characterizing ionospheric effects on communications, satellite drag, and missile reentry dynamics, and for understanding the possibility of covert testing of military weapons systems.

---

* Presented at the Second International Airborne Remote Sensing Conference and Exhibition, San Francisco, California, 24-27 June 1996.

MASTER

DISTRIBUTION OF THIS DOCUMENT IS UNLIMITED

DISCLAIMER

Portions of this document may be illegible in electronic image products. Images are produced from the best available original document.

Radiation-cloud interactions are the dominant uncertainty in the current atmospheric climate models. This is illustrated (Cess, et al, 1989) by a comparison of the sensitivity parameter from 14 leading General Circulation Models (GCMs) used to study the earth's climate system. Even though these models predict similar temperature changes for the case of no clouds, when clouds are included, as in the real world situation, the predicted changes vary by a factor of three.

Reduction of this uncertainty in radiation-cloud interaction is a top scientific priority of not only the ARM program but also of the US Global Change Research Program (USGCRP). While the ARM program measures a number of these parameters from the ground, it was recognized from the outset that other key parameters were best measured in the atmosphere. These important airborne measurements include: (1) The radiation flux throughout the troposphere, which drives atmospheric circulation; (2) cloud properties, from which GCMs calculate the atmospheric heating; (3) the distribution of upper tropospheric water-vapor, a major radiative contributor, and (4) high-altitude flux measurements to calibrate existing satellite-borne sensors. There has also been considerable interest in determining if cloudy atmospheres absorb more shortwave radiation than predicted by current models.

Measurement of these properties at the tropopause for multiple days is beyond the capability of manned aircraft. Major studies by the JASON, DOE, and NASA have called attention to the potential of using defense technology to develop miniature, accurate, UAV-compatible instruments for atmospheric profiling. The MPIR is such an instrument. By appropriate spectral band selections it can measure a wide variety of parameters not only for climate modeling but also for indirect calibration of satellite instruments. A complete description of the methodologies used for these measurements exceeds the scope of this paper. The details can be found in the ARM-UAV Science and Experiment Plan for the 1996 Flight Series (SNL/CA, 1996)

2.0 OPTICAL DESIGN

2.1 BASIC DESIGN

Each of the nine spectral channels consists of a linear detector array operating in a pushbroom mode with optics designed to provide a ±40° across-track field-of-view (FOV). The 256-element long-wavelength detector arrays as well as the short-wavelength 512-element arrays are 25.6 mm long. The optics are all reflective and derived form the SEAL design (Owen, 1990). This provides good aberration correction over an annular ring and results in a curved image footprint on the ground. Each spectral band is in a self-contained module, and all of the modules are aligned to provide co-registered footprints.

The elements of a detector module are illustrated in Figure 1. The light from a scene below the detector passes through (i) an entrance window that protects the instrument from the outside environment; (ii) a chopper used for calibration; (iii) an aspheric convex mirror; (iv) an aspheric concave mirror; (v) a flat fold mirror which also serves as the aperture stop; (vi) a second concave mirror that is rotationally symmetric surface to the first concave element; (vii) a second fold flat which provides a physically accessible image plane; (viii) a sensor window which forms a vacuum seal; (ix) a cooled, narrow-band spectral filter; (x) a cold stop; and arrives finally at (xi) the detector array. The first four mirrors have a common axis of symmetry, which is tilted by 55° from the center of the FOV. The system is f/3.5, with a 5 mm on-axis entrance pupil diameter. The system is nearly telecentric in image

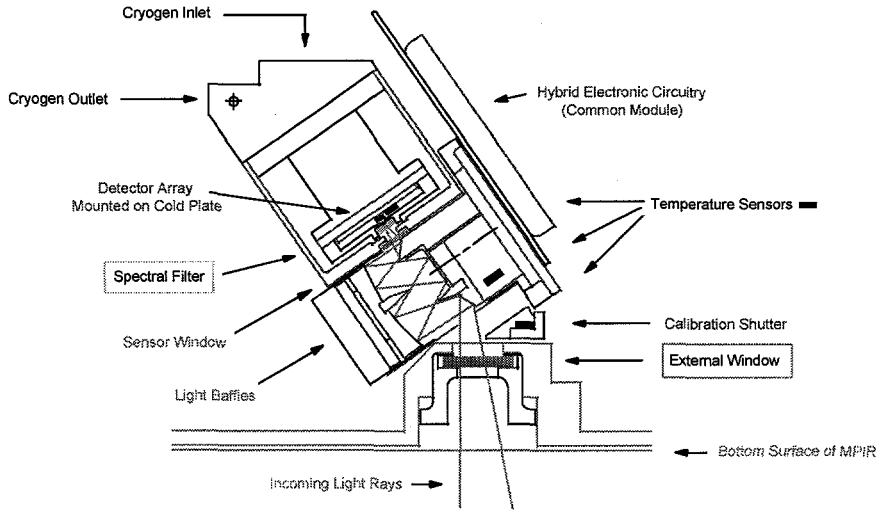

Figure 1 : Schematic of Detector Module Design

space; the interference filters therefore operate at near normal incidence over the entire FOV. The external windows are heated slightly to prevent condensation on descent from high altitudes.

For the shorter wavelengths, the image quality is limited by geometric aberrations. The highest resolution channel uses a Si detector array with 50 μm square pixels. The design is such that 86% of the energy from a collimated, visible input beam is contained within one of these Si pixels. At the longer wavelengths, the array size has been chosen to match the diffraction limited performance, with 86% of the energy from a point image falling within a 100 μm square pixel at a wavelength of 11 μm.

2.2 DISTORTION

The optical design results in large amounts of both pupil and image plane distortion. The pupil distortion is such that the pupil size increases with off-axis distance, an effect that helps to counteract the cosine falloff and thus tends to reduce the dynamic range required within the FOV. Barrel distortion in the image plane has multiple consequences, which are actually beneficial. By adjusting the lateral position of the focal plane perpendicular to the direction of flight, the barrel distortion can be used as an alignment aid to compensate for slight magnification variations or overall array length differences. The instantaneous-field-of-view (IF0V) on the ground varies as a function of field position, but this variation is actually less than the variation from a comparable whiskbroom system. The IFOV of a single pixel, perpendicular to the direction of flight is 2.8 mrad on-axis and 2.5 mrad at the edge of the FOV for a 512-element channel. If the earth were flat, this would translate to 57 and 86 m IFOV footprints, respectively, from a 20 km altitude. The IFOVs are doubled in size for the low-resolution 256-element channels.

For a linear detector array, the distortion results in a curved footprint in the across-track direction (Figure 2). The object space IFOV for a pixel at the edge of the field has an along-track angular displacement of 11.4°. The post-flight image reconstruction process is used to re-map the curved scan lines onto a Cartesian grid. The individual pixels do not overlap in the across-track directions. However,

the spacing between consecutive rows on the ground is dependent of the ground speed of the aircraft. The 256-element data is read out at a fixed rate of 2 data rows per second which gives minimal overlap for a 200 m/sec aircraft ground speed from a 20 km altitude.

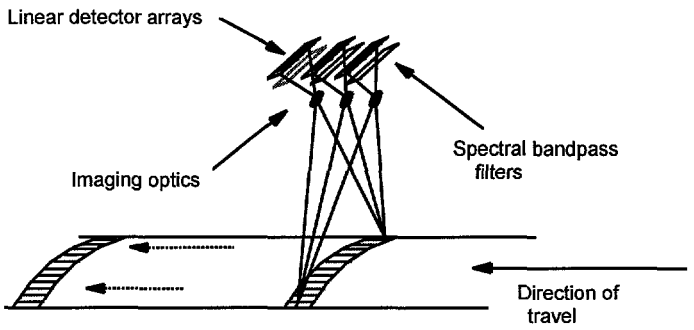

Figure 2: Schematic Showing Pushbroom Imaging and Curved Ground Footprint

2.3 SPECTRAL BANDS

Spectral bands between 0.4 and 12 microns are defined by cooled interference filters. The detector modules use either Silicon, InGaAs, InSb, or HgCdTe detector arrays depending upon the wavelength. Table 1 lists the channels chosen to answer tropospheric cloud questions along with the derived data products. Figure 3 illustrates these bands on a 20-km to sea-level plot of atmospheric transmittance. Each channel is independent, with its own detector array, filter, reflective optics, and electronics

Table 1: Spectral Channels Currently Planned and Their Derived Data Products

Wavelength μm	Derived Data Products
0.62 - 0.67	Cloud identification, amount, thickness, particle size, and phase. Ground reflectance
0.86 - 0.90	Cloud identification and amount, ground reflectance
1.36 - 1.39	Upper tropospheric water vapor, daytime cirrus detection
1.58 - 1.64	Cloud microphysics and phase
2.11 - 2.22	Cloud particle size, and phase
3.55 - 3.93	Cloud particle size, microphysics, and phase.
6.54 - 6.99	Cloud top temperature and height
8.40 - 8.70	Cloud identification and amount, nighttime cirrus, cloud and surface temperatures
10.3 - 11.3	Cloud identification and amount, nighttime cirrus, cloud and surface temperatures

(Figure 4). The digital data from each module is communicated to the main processor in a common format allowing any combination of module types to be assembled into a complete system. As illustrated in Figure 5, a fully populated MPIR contains nine modules kinematically mounted on a common baseplate in a three by three array. This modularity allows a single system design to be used for applications which have different detection wavelengths: cloud radiometry, crop assessment, detection of environmental contamination, etc.

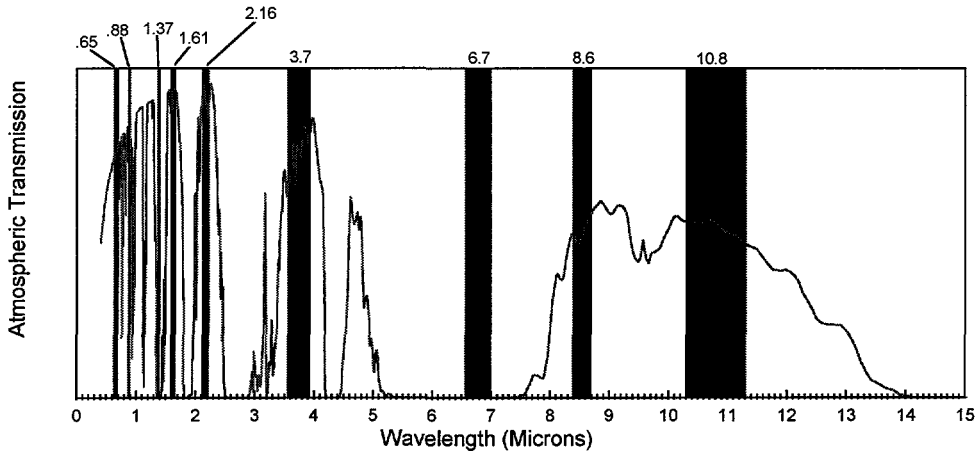

Figure 3: MPIR Spectral Bands Superimposed on Spectral Atmospheric Transmission Profile

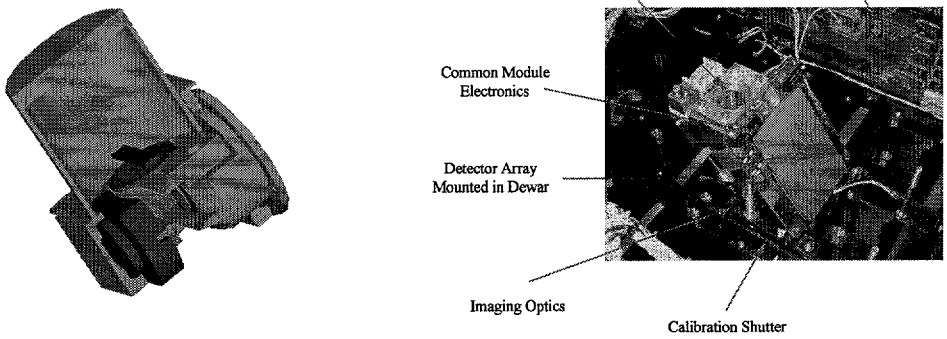

Figure 4: Solid Model of Detector Module Shown (right), Photograph of Module (left)

2.4 LABORATORY CALIBRATION

MPIR will be calibrated at the Los Alamos National Laboratory optical and infrared calibration facility. Calibration goals are 1% (1-σ) uncertainty in the absolute radiance calibration for the long-wavelength infrared (LWIR) and 3% (1-σ) uncertainty for the visible/short-wavelength infrared

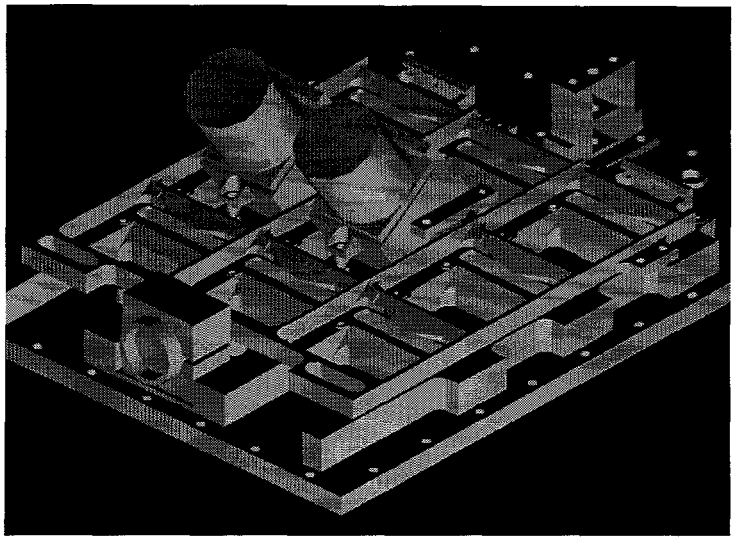

Figure 5: Solid Model Showing Two Detector Modules Located on Baseplate

(VIS/SWIR) region. A grating spectrometer (with a wavelength accuracy of 0.1 nm) will be used in conjunction with NIST-calibrated reference detectors (a Silicon trap photodiode for the VIS/SWIR channels and a composite bolometer and/or cryogenic cavity radiometer for the longer wavelengths) to accurately characterize the end-to-end relative spectral response. MPIR will then be calibrated against standard reference sources of known spectral output; namely, a NIST-designed and calibrated wide-aperture blackbody for the LWIR, and an integrating sphere source for the SWIR. The calculated emissivity of the NIST fluid-bath blackbody is 0.9997 with 1-σ uncertainty of 0.0003 over the MPIR LWIR spectral range. The total temperature uncertainty is 5 mK. The SWIR source radiance uncertainty is 1-2%.

An LN_2-cooled temperature-controlled enclosure capable of simulating the temperature gradients MPIR will experience on the aircraft has been constructed for use in the LWIR calibration. The two water vapor channels, at 1.37 and 6.7 μm, require that the calibration pathlength between the sources and MPIR be purged with dry nitrogen. The quality of the purge will be monitored during calibration by measuring the H_2O infrared absorption lines in a path through the purged area using a fourier transform infrared spectrometer referenced to a vacuum path of the same length. The modulation transfer function, scattered light susceptibility, and polarization sensitivity of MPIR will also be characterized. Finally, to ensure that the calibration is maintained, field calibration sources (an integrating sphere for the VIS/SWIR and a blackbody for the LWIR) will be used immediately before and after each flight to detect and correct for any long-term calibration drifts.

3.0 MECHANICAL DESIGN

3.1 PHYSICAL DIMENSIONS

The MPIR sensor consists of two parts (Figure 6): the main sensor box containing all of the optical modules and associated electronics, and an external dewar which nominally holds five liters of LN_2 for the cryogenic system. The size and configuration of the external dewar depends on the particular UAV mission planned. The system as pictured has a mass of 30 kg and consumes 50 Watts of electrical power.

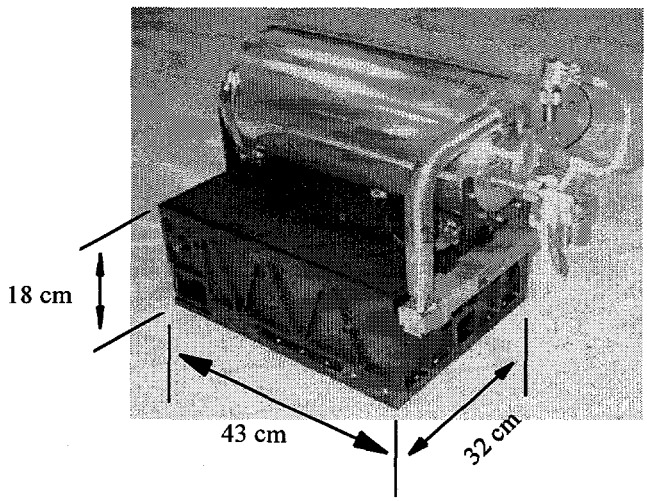

Figure 6: MPIR System (black) with Storage Dewar (silver) Configured for an EGRETT Aircraft.

3.2 DIAMOND-TURNED OPTICS

A goal of the mechanical design was to maintain identical optical properties between modules, thus allowing interchangeability. Diamond-turning of all critical surfaces within each optics module achieved a high degree of similarity, reduced the cost of individually figuring each element, and allowed for a mechanical "bolt-together" alignment. The first and third mirrors were made with two cuts of the same substrate while the second and fourth mirrors are physically the same surface of rotation. After diamond-turning each optic was nickel plated, diamond-turned again, and post-polished under interferometric control. The optics for the shortest wavelength bands are silver coated while the longer wavelength units are gold coated.

3.3 CHOPPER

A calibration chopper oscillates in a horizontal plane below the modules. Each chopper blade surface is coated with a high-emissivity coating (Orlando Black™) to provide a dark reference for the short wavelength channels and a calibration temperature reference for the thermal channels. The chopper oscillates at 4 Hz to provide alternate open- and closed-shutter data collection. Its blades are thermally isolated from the outside environment by a low emissivity optical window and the temperature

of each chopper blade is precisely monitored by an embedded sensor . All of the chopper blades are mounted together on a resonate, torsionally-suspended, momentum-compensated platform and driven by a voice-coil actuator. The chopper is the open, rectangular structure below the detector modules illustrated in Figure 5.

3.4 CRYOGENIC SYSTEM

Temperature regulation of the visible detectors as well as cryogenic cooling for the long-wavelength infrared modules is provided by a liquid nitrogen system. The stored cryogen is sufficient to operate the system for multi-day missions. A single line from the dewar transports the nitrogen to a manifold, were the flow is fed to each detector module through internal transfer hardware (Figures 6 and 7). The Silicon, InGaAs, InSb, and HgCdTe detector arrays will be operated at temperatures of 255 K, 195 K, 80 K, and 80 K respectively. Temperature regulation of 0.5 K at each focal plane is achieved by microprocessor control of a variable impedance solenoid valve on the LN_2 outlet of each module. The exhausted nitrogen gas is used as a dry purge of the main sensor box. Figure 7 shows a single module (center) attached to its cryogen transfer line. (The modules on left and right are not in place.) The in-line flexible bellows allows adjustment for optical alignment.

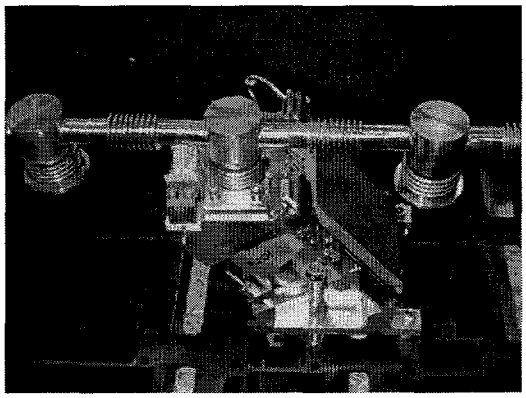

Figure 7: Typical Installation of a Cryogenic Transfer Line (one of three)

4.0 ELECTRICAL DESIGN

Electronics is associated with each detector module which performs the necessary detector signal conditioning and readout functions. Communication between each module and the main microprocessor is via a synchronous serial data link for data queuing and communications (Figure 8).

The dynamic range of each array is such that a full 0.25 second integration period would cause saturation. Therefore, each array is read out several times during the 60 ms data collection interval and multiple readings are averaged to give a single 12-bit data value. Similar averaged readings are taken

with the chopper open and closed to correct for any calibration drifts during flight. Table 2 lists the Noise-Equivalent-Delta-Radiance (NEΔR) in mW/m^2-sr for bands 1-6 and the Noise-equivalent Noise-Equivalent-Delta-Temperature (NEΔT) for bands 7, 8, and 9.

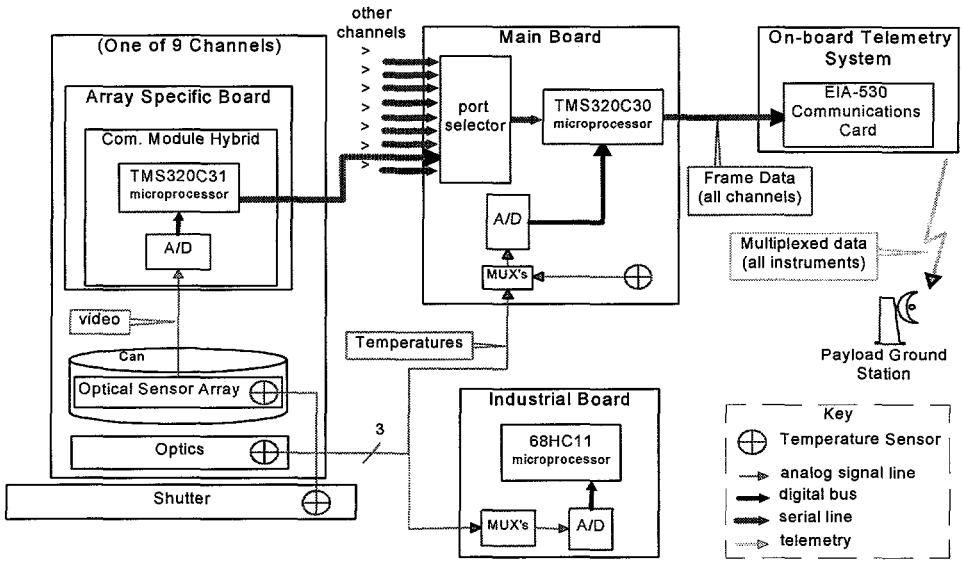

Figure 8: MPIR Data Flow Schematic.

Table 2: Number of Subscans Per Data Row for Each Channel Along with NEΔR and NEΔT.

Band μm	Detector	Pixel size, μm	Scans per data row	Band origin	NEΔR and NEΔT
0.62 - 0.67	Si	50	6	MODIS 1	6.1
0.86 - 0.90	Si	50	12	--	3.0
1.36 - 1.39	InGaAs	50	28	MODIS 26	0.9
1.58 - 1.64	InGaAs	50	28	AVHRR 3a	1.2
2.11 - 2.22	InGaAs	100	6	MCR 6	0.6
3.55 - 3.99	InSb	100	6	AVHRR 3b	0.5
6.54 - 6.99	InSb	100	60	GOES 12	0.04
8.40 - 8.70	HgCdTe	100	60	MODIS 29	0.03
10.3 - 11.3	HgCdTe	100	60	AVHRR 4	0.03

The output data is a serial, digital data stream at a rate of 80 kbps. A ground-based telemetry station or an onboard data recorder is used to receive and store the raw data. A personal computer can be used for a near-real-time display of collected data on the ground. This 'Quick Look' capability can be used to monitor state-of-health and allows dynamic control of the mission as the situation evolves.

8.0 CONCLUSIONS

MPIR is designed to be a flexible, relatively inexpensive, multi-spectral instrument with a duplication cost in the $1M per copy range. Reconfiguration of its modules for various missions can be accomplished rather inexpensively. A simple filter change would require a few thousand dollars for new interference filter and optical window hardware for each channel changed plus the labor to optically realign the system. At the present time the four shortest wavelength bands are operational and all nine bands are to be completed for flights in the fall of 1996.

9.0 REFERENCES

R. D. Cess, G. L. Potter, J. P. Blanchet, G. J. Boer, S. J. Ghan, J. T. Kiehl, H. Le Treut, Z.-X. Li, X.-Z. Liang, J. F. B. Mitchell, J.-J. Morcrette, D. A. Randall, M. R. Riches, E. Roeckner, U. Schlese, A. Slingo, K. E. Taylor, W. M. Washington, R. T. Wetherald, I. Yagai, " Interpretation of Cloud-Climate Feedback as Produced by 14 Atmospheric General Circulation Models", *Science*, Vol. 245, No. 4917, 4 August 1989

Atmospheric Radiation Measurement-Unmanned Aerospace Vehicle Science and Experiment Plan 1996 Flight Series, Revision 3 - February 6, 1996, Program Director Office, Global Climate Change and Remote Sensing Project Office, Sandia National Laboratories, Livermore, California

R. Calvin Owen, "Easily fabricated wide angle telescope", In *International Lens Design Conference* , George N. Lawrence, editor, Monterey, California, SPIE Vol. 1354, pp 430-433, June 1990.

10.0 ACKNOWLEDGMENTS

MPIR is being developed for the DOE's ARM/UAV program with funding from the Strategic Environment Research and Development Program under direction of the ARM/UAV Technical Director, Dr. John Vitko, Sandia National Laboratories/California, Department 8102. This work was supported by the United States Department of Energy under Contract DE-AC04-94AL85000.

DISCLAIMER

This report was prepared as an account of work sponsored by an agency of the United States Government. Neither the United States Government nor any agency thereof, nor any of their employees, makes any warranty, express or implied, or assumes any legal liability or responsibility for the accuracy, completeness, or usefulness of any information, apparatus, product, or process disclosed, or represents that its use would not infringe privately owned rights. Reference herein to any specific commercial product, process, or service by trade name, trademark, manufacturer, or otherwise does not necessarily constitute or imply its endorsement, recommendation, or favoring by the United States Government or any agency thereof. The views and opinions of authors expressed herein do not necessarily state or reflect those of the United States Government or any agency thereof.